Single-Stage Buck-Boost Transformerless Inverter for Grid-Connected solar PV Systems

[1]S. Suganya, [2]S. Abinath, [3]S. Karthikeyan, [4]L. Krishna Kumar, [5]M. Hariharan

[1]Assistant Professor – Dept of EEE – Paavai Engineering College,
[2,3,4,5]Student – Dept of EEE – Paavai Engineering College.

Abstract:This paper presents a single-phase current transformer (BBTI) topology for single-phase grid-tied solar PV applications. In this topology, Input PV source shares common ground with neutral pores that eliminate leakage currents. In addition, the proposed topology has the ability to improve the tracking body peak power point even more variety of inputs PV voltage. Other features of the proposed topology is the supply uses only one energy-saving inductor symmetrical operation in two half cycles of the network. In addition, two of the five switches of the proposed topology operate at line frequency and therefore exhibit low commutation loss and three other switches are moved in any order process with low transmission loss. A simple sine-triangle pulse width modulation strategy is proposed for control the proposed inverter topology is analyzed throughout the work terms and explained in detail. The exam was conducted 300W laboratory prototype and key findings included in the paper presenting the proposed system providing high efficiency with low THD in output current.

I) Introduction:

Typically, PV-fed transformerless inverters suffer from leakage current [1]. To overcome the leakage current Researchers have developed many PV-fed transformerless inverter topologies and control strategies[2], [3]. For example, a central or off-grid inverter configuration connected to the grid consists of rows of PV panels that do not require a charging stage. However, low-voltage PV sources require a step-up stage, which reduces the efficiency of the system. Some studies have found DC-converted inverters fail during low-voltage PV supply or PV supply with shaded conditions [4], [5]. In order to have a wide application range of PV sources, it is recommended to have transformerless inverter topologies with the ability to boost the body [6] - [16]. From this point of view, it can be understood that current researchers prefer to propose a transformerless topology based on suspension [10] - [15]. The authors of [10] proposed to produce a fixed inverter topology suitable for large-scale PV system operation. However, the disadvantage of this topology is that it requires two separate PV sources for each half cycle of the output voltage. In [11], a transformerless topology current booster using only four switches and two input inductors is proposed. In this topology, each input inductor operates on a positive or negative half cycle, which can cause DC current injection. Another disadvantage of this topology is that the current THD is more than 5%, which is higher than the IEEE limit. The author [12] proposed a multiplexed topology with a single input inductor and switch 5. But this topology requires three additional diodes. Although this topology has a single input inductor, a large input capacitor is required to handle the peak power from the PV source. Another disadvantage of this topology is low voltage gain. [13] topology can be used for a Various PV systems. But eight switches and one inductor are required. The number of switches is high reduce efficiency, reliability and increase system costs. A body augmentation is proposed in [14] topology reduces the number of switches (ie five switches). However, this topology requires greater access capacity track solar PV peaks. The topology [14] is also used for various PV systems. In this topology, three switches are switched during each switching cycle, which increases the transmission loss. Another disadvantage of this system is the need for an inductor that carries a large current at the input, which increases the system size, cost, and efficiency. To reduce the number of switches, [15] researchers proposed the current topology with only two switches. But in this topology, there is no symmetrical operation in the positive and negative half cycles of the output voltage. Another disadvantage of this topology is that the voltage at the PV input is higher than the required voltage. Another topology [16] was proposed using a coupled inductor. This topology can provide high voltage gain output, but in this topology three switches are switched in one switching cycle reduce transmission losses and system efficiency. take advantage of the above defects This paper proposes an inverter topology without a step-up transformer with only five switches and a single input inductor at the input. The main advantages of the proposed topology are as follows:

1. Zero leakage due to common terminal shared between PV and grid neutral.
2. small current injection due to symmetry operating in positive and negative half cycles.
3. Fewer switches to manage the system is more reliable and highly efficient.
4. A variety of PV power tracking is possible having a body augmentation procedure.

II) INVERTER TOPOLOGY To be translated Buck-ios:

This section discusses the proposed transformerless inverter topology architecture and technique to work Structure proposal Buck-Boost transformerless inverter topology. The proposed Buck-boost transformer inverter topology (BBTI) is shown in Figure 1. BBTI consists of five control switches S1 to S5, an input inductor 'L', a power diode 'D' and an auxiliary capacitor CA. Of the five switches, S1, S3 and S4 operate at high frequency (ie switching frequency) and S2, S5 operate at line frequency (ie 50Hz). In the BBTI topology (shown in Figure 1), it can be observed that the negative terminal of the PV is directly connected to the neutral of the grid, which completely eliminates the leakage current. BBTI operation pattern for positive and negative half cycle of grid voltage in the case of continuous transmission r (im (ie iL> 0) shown in Fig. 2 (a) - (d) and their corresponding switching conditions are presented in Table-I.

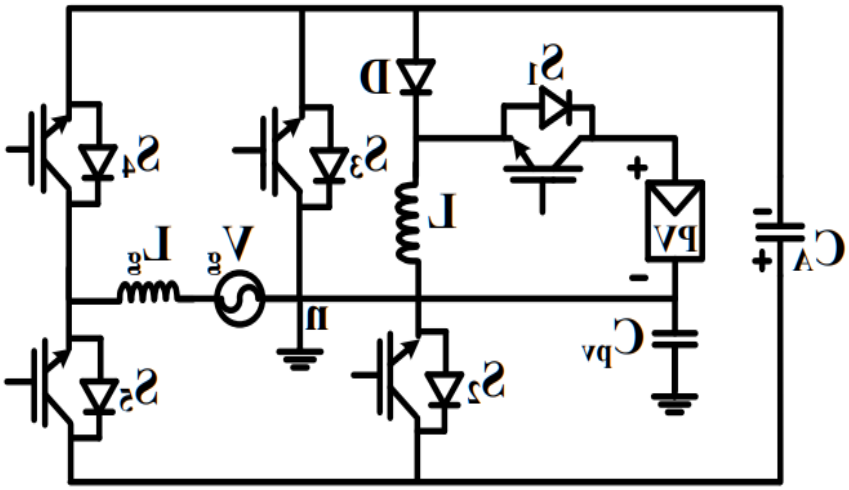

Fig. 1. The proposed buck-boost transformerless inverter (BBTI) topology.

TABLE I. OPERATING MODES CORRESPOND TO SWITCHES STATES

Operation of BBTI		Switches states (1=ON, 0=OFF)						Mode
		S_1	S_2	S_3	S_4	S_5	D	
+Ve half cycle	$i_L>0$	1	0	1	0	1	0	a
		0	0	0	0	1	1	b
-Ve half cycle		1	1	0	1	0	0	c
		0	1	0	0	0	1	d

Continuous Conduction Mode (CCM) of BBTI is mainly divided into four modes (Mode-(a) to Mode-(d)). Corresponding to the positive and negative half cycles of the grid. Mode-(a), Mode-(b) correspond to the positive half cycle and Mode-(c), Mode-(d) correspond to the negative half cycle of the grid (shown in Fig. 2(a)-(d)). The various switching states corresponding to all modes of operation are shown in Table I. The modes of operation of BBTI are explained below for four important modes of operation:

Mode-(a): During this mode, the BBTI provides power to the grid as shown in Fig. As shown in 2(a). In this mode, power switches S1, S3 and S5 are on. The energy storage inductor (L) stores the energy from the PV source through the power switch S1 and the auxiliary capacitor CA to the grid through the switches S3 and S5 in Fig. Energized supplies along the thick lines as shown in Fig. 2(a). All current flowing paths corresponding to this mode of operation are shown in Fig. are highlighted with thick lines as shown in Fig. 2(a).

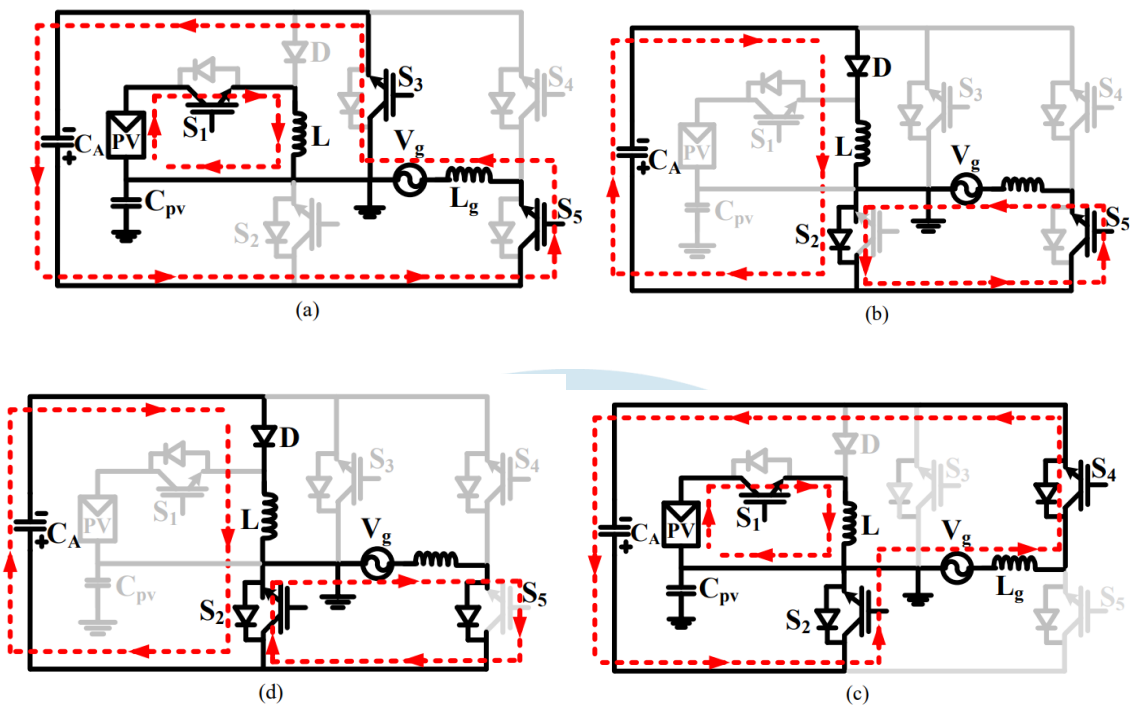

Mode-(b): In this operating mode, power switch S5 is open and all switches are still closed, as shown in figure 2(b). The inductance (L) supplies its stored energy to the auxiliary capacitor CA via a parallel diode shield between diode "D" and S2. The current in the gate inductor "Lg" is free-rotating through the anti-parallel diodes of Switch S5 and Switch S2. All methods that led to such studies are shown in bold lines as shown in Figure 1.2 (b)

Mode-(c): This mode corresponds to powering the grid in the negative half cycle. During this mode, power Switches S1, S2 and S4 are ON. An auxiliary capacitor supplies energy to the grid via AC power S2 and S4 switches. An energy storage inductor stores energy from the input PV source through switch S1. All of them The behavior path corresponding to this mode of operation is shown in Fig. are highlighted with thick lines as shown in Fig. 2(c).

Mode (d): This mode corresponds to the free-running period of the inductor Lg. This is a circuit breaker the residual current switch is opened during shutdown. In this case, the inductor "L" is maintained power for auxiliary capacitor CA through diode D and antiparallel diode of switch S2. The current in the free pole of the inductor Lg passes through the antiparallel diode switch S2 and switch S5. All transmission lines associated with this procedure are indicated by thick lines, as shown in Fig. 2 (d).

B. **Steady-state analysis of the proposed BBTI topology**

To perform steady state analysis of BBTI topology, the following prerequisites are considered.

1) The DC capacitor voltage is constant (that is, the DC capacitor is large)

2) All semiconductor devices are lossless.

3) Parasitic parameters are ignored.

By applying the voltage balance across the inductor (L) the following equation is obtained:

$$\int_{0}^{m_i T_S} V_{pv} dt + \int_{m_i T_S}^{T_S} \left(-V_{C_A}\right) dt = 0 \qquad (1)$$

From (1), the voltage across the auxiliary capacitor (CA) is obtained as

$$V_{C_A} = \left(\frac{m_i}{1-m_i}\right) V_{PV} \qquad (2)$$

The maximum AC output voltage of the BBTI can be expressed as:

$$V_{AC} = m_i \times V_{C_A} \qquad (3)$$

By substituting (2) in (3) the gain of the proposed BBTI can be obtained as

$$G = \frac{V_{AC}}{V_{PV}} = \left(\frac{m_i^2}{1-m_i} \right) \quad (4)$$

C. **Design of energy storage elements of the BBTI topology**

The section presents the design of various energy storage elements of the BBTI topology.

a. Design of energy storage inductor (L)

An energy storage inductor (L) at the input of the BBTI is designed similarly to a conventional buck-boost -DC converter. The value of inductance is chosen such that the BBTI should work in CCM. Selected in CCM the inductance value is greater than the critical inductance (LC) to operate the BBTI. Expression to calculate LC given as:

$$L_C = \frac{(m_i V_{PV})^2}{2 P_o f_S} \quad (5)$$

Where,

mi: Modulation index
VPV: Input PV voltage
Po: Output AC power
fS: Switching frequency

b. Design of auxiliary capacitor (CA)

The output power (Po) and the voltage deviation of the corresponding capacitor are used to calculate the value condenser. Typically, capacitor voltage drift is assumed to be 5%. The expression for calculating the value of the auxiliary capacitor is given as follows:

$$C_A \geq \frac{P_o}{\Delta V_{C_A} \times V_{C_A} \times f_S} \quad (6)$$

Here, CA is the value of the auxiliary capacitor. VCA is the voltage across auxiliary capacitor and ΔVC is the ripple voltage of auxiliary capacitor.

III. MODULATION AND CONTROL STRATEGIES OF THE PROPOSED BBTI TOPOLOGY

The modulation and control strategies of the grid-connected BBTI topology are presented in this section.

A. Modulation and control strategies of the BBTI topology

The proposed modulation strategy of BBTI topology is shown in Figure 3. In this modulation strategy, the modulating waveform is (Vmsin(wt)) and it is the absolute (|Vmsin(wt)|), inverse (-Vmsin(wt)) waveform. is compared with the triangular waveform (Vtr) to generate the switching pulse at the switches (S1 to S5). Operates on switches S2 and S5 Line frequency (ie 50Hz) as shown in Fig 3. The switching pulse at S3 is generated by comparing Vmsin(wt) to one. Triangular waveform (Vtr). Similarly switching pulses across switches S1, S4 are generated by comparing |Vmsin(wt)| and -Vmsin(wt) with triangular waveform Vtr. The proposed BBTI topology feeds power from the input PV source in grid using current control strategy [11]. The maximum power point of the input solar PV source is tracked using the perturb and monitor MPPT algorithm [7].

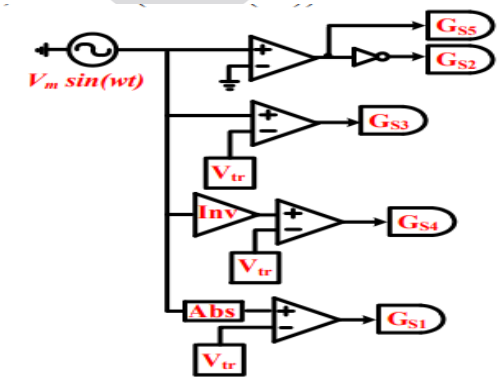

B. Comparison of the proposed BBTI topology with existing buck-boost transformerless inverter topologies.

The proposed BBTI topology suffers from low switching and transmission losses due to the number of switches (only three) operate at high frequency and with several switches (only three) during all operating modes Figure 2 (a)–(d)). Therefore, BBTI topology has lower switching and transmission losses compared to step-up inverterless transformerless topologies, which increases the efficiency of the system. The details Comparison of the proposed BBTI topology with the existing boost-based transformerless inverter topology

Given in Table II.

TABLE II COMPARISON OF BBTI WITH OTHER BUCK-BOOST TRANSFORMERLESS INVERTER TOPOLOGIES:

Parameters	BBTI	Ref [11]	Ref [13]	Ref [15]
Number of switches	5	6	5	5
Number of diodes	1	0	2	0
Number of inductors	1	1	2	1
Number of capacitors	1	1	0	1
DC offset	No	No	Yes	Yes
% THD	3.31	<5	<5	4.5

IV. Simulation and experimental results of grid-connected BBTI topology

This section presents the simulation and experimental results of the grid-connected BBTI topology.

A. Simulation results:

A grid-connected BBTI system is simulated in MATLAB/Simulink for a 300W power rating. The system parameters used for MATLAB simulations are given in Table-III. The voltage rating of the input solar PV source is assumed to be 75V. The proposed BBTI topology feeds the maximum available power from the PV source to the grid with a THD of 3.31%. Some of the main simulated waveforms like grid voltage (Vg), grid current (IO), input inductor current (iL) and auxiliary capacitor voltage (VCA) are shown in Fig.4.

TABLE III SYSTEM PARAMETERS FOR SIMULATION STUDIES

Power rating	300W
Switching frequency	10kHz
Input voltage	75V
Input inductor (L)	115μH
Auxiliary capacitor(C_A)	50 μF
Output inductor (L_g)	1mH
Filter capacitor (C_f)	10 μF
DSP Controller	TMS320F28335

Fig. 4. The simulated waveforms of the PV fed grid-connected BBTI topology; (a) the grid voltage (Vg); (b) Current through grid (Ig); (c) Current through input inductor current (iL); (d) Voltage across auxiliary capacitor (VCA).

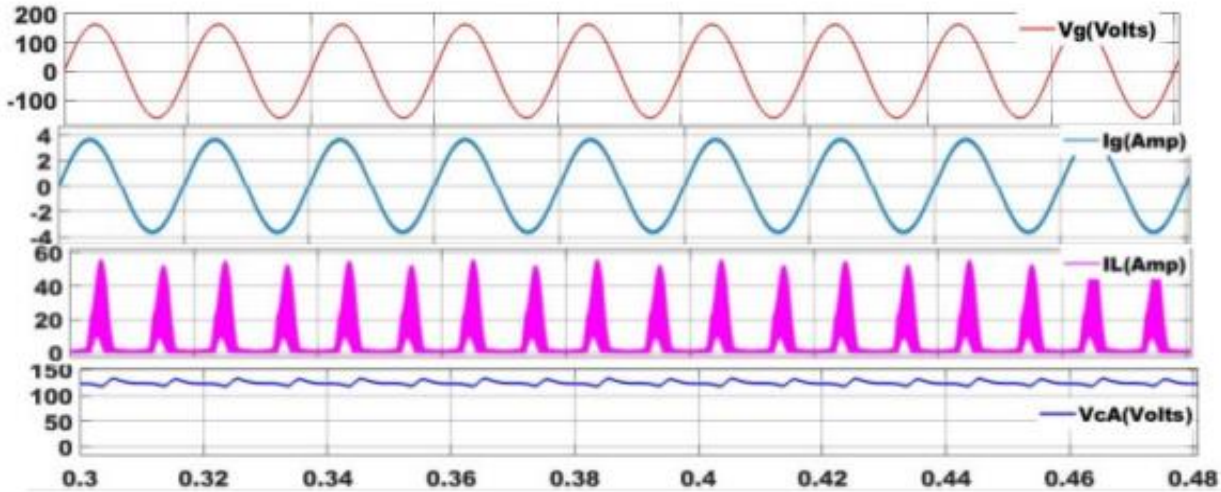

B. Experimental results:

The grid-connected BBTI topology is validated in a laboratory prototype for a power rating of 300W. It is important,the test waveform including gate voltage (Vg), gate current (Ig), input inductor current (iL) and auxiliary capacitor voltage (VCA) is shown in Figure 5. It can be observed from the proposed test BBTI provides a good quality feed to the grid with a THD of 3.8%.

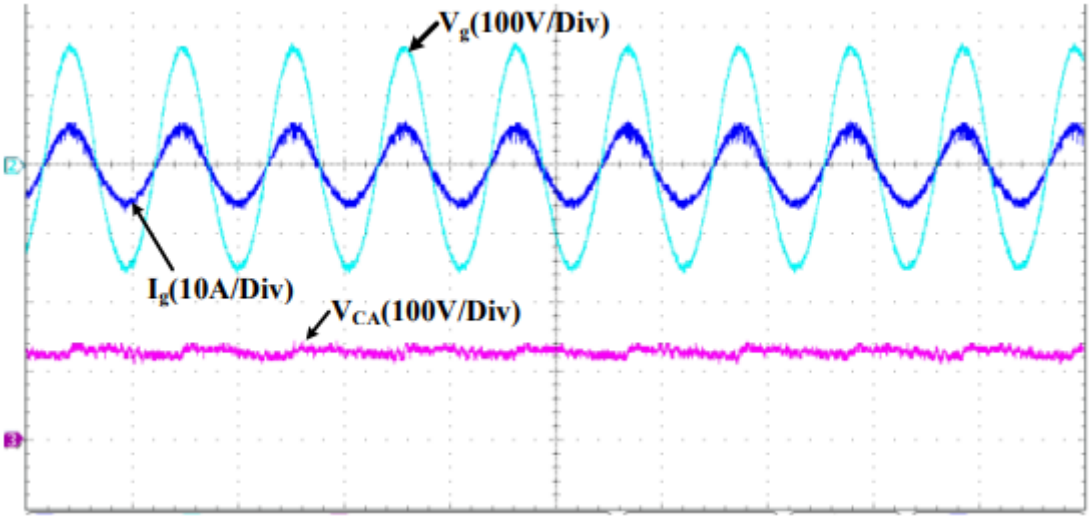

Fig. 5. The experimental grid voltage (Vg), grid current (Ig) and auxiliary capacitor voltage (VCA) of PV fed grid-connected BBTI topology

V. CONCLUSIONS:

A novel buck-boost transformerless inverter topology was proposed, analyzed and experimentally validated. Results It has been verified that the BBTI topology injects zero leakage current and negligible DC current into the grid for grid-connected PV applications. BBTI's buck-boost property can have maximum power points tracked for PV under wide voltage variation. The BBTI was tested at a switching frequency of 10 kHz and it is observed that the current THD is 3.8% which is in good agreement with IEEE standards.

REFERENCES :

1. E. Gubia, P. Sanchis, A. Ursua, J. Lopez, and L. Marroyo, "Ground currents in single-phase transformerless photovoltaic systems," in Progress in Photovoltaics: Research and Applications. New York: Wiley, pp. 629-650, Nov. 2007.
2. Gubía. E, Sanchis. P, Ursúa. A, López. J and Marroyo. L, “Ground currents in single-phase transformerless photovoltaic systems,” in Progress in Photovoltaics: Research and Applications. NewYork: Wiley, pp. 629- 650, 2007.
3. O. Lopez et al. “Eliminating ground current in a transformerless photovoltaic application,” IEEE Trans. on Energy Conversion, vol. 25, no. 1, pp. 140–147, Mar. 2010.
4. D. Barater, E. Lorenzani, C. Concari, G. Franceschini, and G. Buticchi, “Recent advances in single-phase transformerless photovoltaic inverters,” IET Renew. Power Gener., vol. 10, no. 2, pp. 260–273, 2015.
5. W. Yu, 1. S. Lai, H. Qian, C. Hutchens, J. Zhang, G. Lisi, A. Diabbari, G. Smith and T. Hegarty, "High-efficiency inverter with H6-type configuration for photovoltaic non-isolated AC module applications," Proc. IEEE Appl. Power Electron. Conf. Expo., pp.1056 -1061, Feb. 2010.

6. N. Kasa, H. Ogawa, T. Iida, and H. Iwamoto, “A transformerless inverter using buck-boost type chopper circuit for the photovoltaic power system,” in Proc. IEEE Int. Conf. Power Electron. Drive Syst., 1999, pp. 653–658.
7. S. Jain and V. Agarwal, “A single-stage grid-connected inverter topology for solar PV systems with maximum power point tracking,” IEEE Trans. Power Electron., vol. 22, no. 5, pp. 1928–1940, Sep. 2007.
8. B. S. Prasad, S. Jain, and V. Agarwal, “Universal single-stage gridconnected inverter,” IEEE Trans. Energy Convers., vol. 23, no. 1, pp. 128–137, Mar. 2008.
9. H. Patel and V. Agarwal, "A single-stage, single-phase transformerless doubly grounded grid-connected PV interface," IEEE Trans. Energy Conversion, vol. 24, pp. 93–101, Mar. 2009.
10. Y. Tang, X. Dong, and Y. He, “Active buck-boost inverter,” IEEE Trans. Ind. Electron., vol. 61 no. 9, pp. 4691–4697, Sep. 2014.
11. P. Chamarthi, M. Rajeev, and V. Agarwal, “A novel single-stage zero leakage current transformerless inverter for grid-connected PV systems,” in Proc. IEEE 42nd Photovolt. Spec. Conf., New Orleans, LA, USA, Jun. 2015, pp. 1–5.
12. N. V´azquez, M. Rosas, C. Hern´andez, E. V´azquez, and F. J. Perez-Pinal, “A new common-mode transformer-less PV inverter,” IEEE Trans. Ind. Electron., vol. 62, no. 10, pp. 6381–6391, Oct. 2015.
13. T. Sreekanth, N. Lakshminarasamma, and M. K. Mishra, “A single-stage grid-connected high gain buck-boost inverter with maximum power point tracking,” IEEE Trans. Energy Convers., vol. 32, no. 1, pp. 330–339, Mar. 2017.
14. A. Kumar and P. Sensarma, “A four-switch single-stage single-phase buck-boost inverter,” IEEE Trans. Power Electron., vol. 32, no. 7, pp. 5282–5292, Jul. 2017.
15. V. Gautam and P. Sensarma, “Design of Cuk-derived transformer-less common-grounded PV micro-inverter in CCM,” IEEE Trans. Ind. Electron., vol. 64, no. 8, pp. 6245–6254, Aug. 2017.
16. T. Sreekanth, N. Lakshminarasamma, and M. K. Mishra, “A single-stage grid-connected high gain buck-boost inverter with maximum power point tracking,” IEEE Trans. Energy Convers., vol. 32, no. 1, pp. 330–339, Mar. 2017.